EuroIntervention

Essentials of quantitative angiography for bifurcation lesions

Chrysafios Girasis, MD; Robert-Jan van Geuns, MD, PhD; Yoshinobu Onuma, MD; Patrick W. Serruys*, MD, PhD

Interventional Cardiology, Erasmus MC, Rotterdam, The Netherlands

The authors have no conflict of interest to declare.

Introduction

Visual estimation of vessel diameter and lesion length supported by balloon predilation (known length and diameter) has been a common strategy, when final stent implantation is anticipated. Quantitative coronary angiography (QCA) being highly accurate and reproducible[1,2] can refine the visual estimate and provide several important parameters which have been accepted as surrogate endpoints in many clinical studies on new PCI technologies[3-5]. However, stand-alone percent diameter/area stenosis measurements derived from conventional (single-vessel) two-dimensional (2-D) QCA analysis fail to predict the functional significance of coronary vessel obstruction[6,7]. This holds even more for the analysis of bifurcation lesions[8], where the discrepancy in vessel size proximal and distal to the carina (step-down phenomenon) results in stenosis being overestimated in the distal branches and underestimated in the proximal main vessel (PMV)[9]. Dedicated 2-D bifurcation software algorithms have been developed recently[10-12] in order to make up for the shortcomings of 2-D single-vessel QCA by reporting angiographic parameters separately for the PMV and each of the distal branches.

The proximal and the distal branches of a single bifurcation often do not lie on a single plane; thus vessel overlap and foreshortening together with the lesion eccentricity may compromise the results of 2-D angiographic analysis[13]. In the last 10 years evidence has accumulated that three dimensional (3-D) angiographic reconstruction is accurate, precise and reproducible[14-18]. Reduced time requirements for a single 3-D reconstruction facilitates real-time analysis; single-vessel as well as bifurcation lesions[19,20] can be reconstructed and analysed via dedicated QCA algorithms.

In this short review we will attempt to emphasise the relative merits of bifurcation QCA compared to visual assessment, report on the options currently available for 2-D and 3-D bifurcation QCA analysis and outline the challenges yet to be addressed.

Bifurcation lesions: visual assessment vs. QCA

A first requirement for the accurate and precise interpretation of a bifurcation lesion is the acquisition of high quality images. Whereas single-vessel lesions are usually acquired and assessed in two orthogonal views, optimal visualisation of a bifurcation lesion, and especially the ostium of the side branch (SB), is increasingly challenging. Absence of vessel overlap, minimal foreshortening and widest possible angle between the main vessel and the SB usually can be found together in one single best view[11]. In the interest of reproducibility and possible 3-D reconstruction, an added 1-2 projections separated by an angle ≥30°, should be acquired according to the aforementioned criteria.

In accordance with the European Bifurcation Club (EBC), a bifurcation lesion is defined as a coronary artery narrowing adjacent to, and/or involving, the origin of a significant SB; significant is a SB that you do not want to lose[21]. The current consensus in bifurcation lesion classification is the one proposed by Medina[22]. The PMV, the distal main vessel (DMV) and the SB are visually adjudicated for the presence of narrowing in excess of 50%; every vessel segment, following the same order, gets appointed with a binary value of 1 or 0 according to the presence or absence of significant stenosis, respectively. Lesions with Medina class (1,1,1), (1,0,1) and (0,1,1), where both the main vessel and the SB display significant stenosis, are designated as "true" bifurcation lesions.

** Corresponding author: Thoraxcenter, Ba-583, 's Gravendijkwal 230, 3015 CE Rotterdam, The Netherlands*
E-mail: p.w.j.c.serruys@erasmusmc.nl

A more rigorous Medina classification would have to be based on percent diameter stenosis (DS) values derived from quantitative analysis. Already in the early 80s, Serruys et al[23] reported a discrepancy between visual and QCA estimates of DS values in single-vessel lesions, visual estimate systematically overestimating severe QCA-assessed stenoses by almost 10%; similar studies corroborated this finding[24,25]. The large intra- and inter-observer variability of visual estimate (SD up to 18%) has been a consistent finding since the late 70s[26-28]. In order to evaluate the accuracy and precision of DS visual estimates among experts in the field of bifurcation lesions a survey was carried out during the fifth annual meeting of the European Bifurcation Club, held in Berlin in 2009[29]. Thirty-six experts assessed visually the degree of percent diameter stenosis in cine images of five true bifurcations lesions in precision manufactured plexiglas phantoms; the evaluated bifurcation lesions differed in vessel diameter, angulation and stenosis severity. In total 24.6% of the reported visual assessments were exact, 25.9% being under- and 49.4% over-estimations (Figure 1). The DS in the PMV was usually underestimated, whereas it was almost consistently overestimated in the DMV and the SB. Visual assessments among this body of experts were considerably variable, almost 3-fold compared to the performance of dedicated 2-D bifurcation QCA software.

This diminished accuracy of visual assessments can be explained by the intuitive way even experienced operators interpret ostial lesions of distal bifurcation branches, wherein distal vessel size and consequently stenosis severity is overestimated by referring to the PMV segment. By the same principle PMV lesions can be underestimated by referring to the distal branches' size. These phenomena are also reflected in the way single-vessel QCA analysis has been applied in the bifurcation lesions; manual extension of vessel contours from the SB/DMV into the PMV assumes smooth vessel tapering and not the step-down phenomenon (acute tapering) inherent in a bifurcation[9]. In fact, the true size of the PMV, DMV and SB is dictated by scaling laws, such as Murray's Law ($[PMV]^3 = [DMV]^3 + [SB]^3$) or the more refined HK model ($[PMV]^{7/3} = [DMV]^{7/3} + [SB]^{7/3}$)[30], both based on the minimum energy hypothesis and conservation of energy under steady-state conditions. The step-down in reference vessel diameter (RVD) distal to the carina can be also described by the simplified law of Finet[31], wherein PMV=0.678*(DMV+SB).

Dedicated 2-D bifurcation QCA software

Dedicated 2-D bifurcation QCA algorithms have been recently developed and integrated into the Cardiovascular Angiography Analysis System (CAAS) (Pie Medical Imaging, Maastricht, The Netherlands)[10,12] and QAngio XA (Medis medical imaging systems, Leiden, The Netherlands)[11] in order to make up for these shortcomings. In both software packages, path-lines are drawn between user-defined delimiter points in PMV, DMV and SB at the largest possible distance from the bifurcation to be analysed, usually between adjacent bifurcations; vessel contours are then traced through edge-detection (ED) techniques following minimum cost algorithms.

QAngio XA contains two bifurcation models, one for T-shaped bifurcations and one for Y-shaped bifurcations, following criteria based on the angulation and diameter ratio between the DMV and the SB. The outer contours of all vessel segments are defined as a whole with no interpolation across the SB. Conventional straight vessel analysis is followed for the arterial diameter calculation, except for the SB in T-shaped bifurcations, where Medis ostial analysis is applied. The T model consists in a main vessel with a smoothly tapering RVD function and a SB with its reference displayed by a straight line with a proximal flare corresponding to the mouth of the ostium. In the Y model the bifurcation core is combined with the PMV resulting in a straight RVD function with a distal flare; the two distal vessel segments are displayed separately[11] (Figure 2).

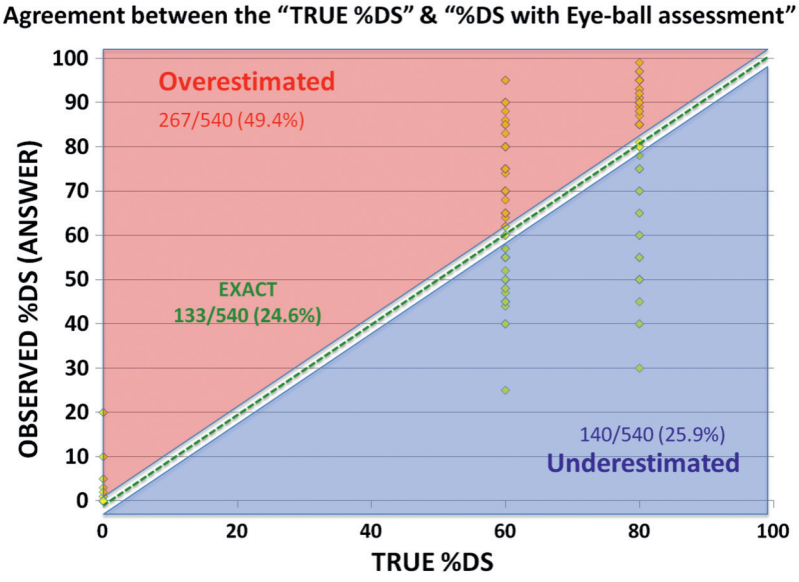

Figure 1. Agreement between visual assessment and true percent diameter stenosis (DS) values in phantom bifurcation lesions. Modified Bland-Altman plot, wherein the dotted green line (line of equality) separates the overestimated from the underestimated assessments. All estimates for the proximal main vessel, the distal main vessel and the side branch are pooled (540 in total) and largely overlapping due to identical values.

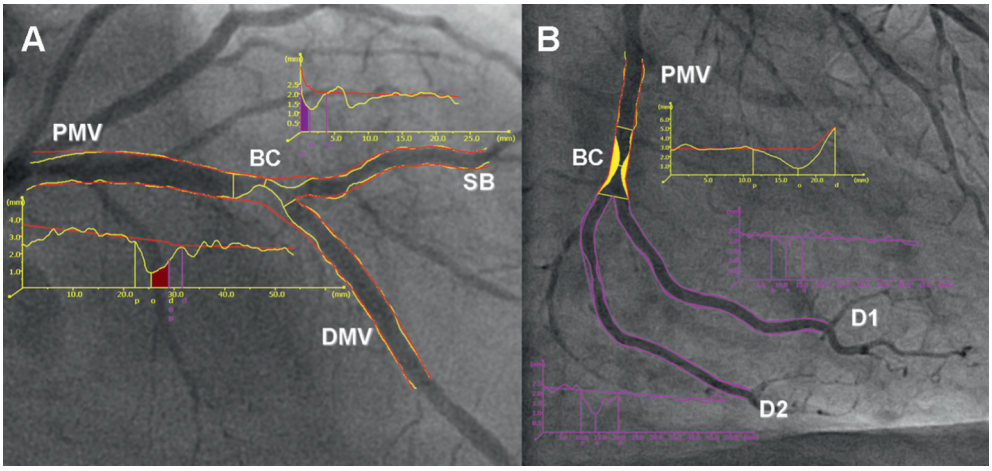

Figure 2. Bifurcation lesion analysis in QAngio XA. A. T-shape analysis. Analysis is performed separately for the main vessel, consisting of the proximal main vessel (PMV), the bifurcation core (BC) and the distal main vessel (DMV), and for the side branch (SB). The main vessel has a smoothly tapering reference vessel diameter (RVD) function (red line in the diameter graphs), whereas in the SB, RVD function is displayed by a straight line with a proximal flare corresponding to the mouth of the ostium (Medis, ostial analysis). B. Y-shape analysis. The bifurcation core is combined with the PMV resulting in a straight RVD function with a distal flare; the two distal vessel segments, D1 and D2, are displayed separately. (Figures were provided by G. Koning, Medis medical imaging systems)

In the CAAS bifurcation QCA software, the bifurcation is delineated by a left, right and middle contour making no further assumptions. An instrumental role is reserved for the point of bifurcation; this is the point, where the centre lines from the vessel segments converge and is defined as the centre of the largest inscribed circle in the bifurcation region, touching all three vessel contours. The polygon of confluence (POC) represents the smallest possible region that behaves differently from a single vessel segment. In the POC the diameter is determined by a "minimum freedom" approach; the RVD function is based on an interpolation technique, assuming a constant curvature within the POC[10]. In the interest of simplification, Serruys et al proposed the extrapolation of the RVD function outside the obstruction boundaries, separately for each vessel segment; RVD for each vessel segment is called by one straight line up until the point of bifurcation[12] (Figure 3).

Both QAngio XA and CAAS algorithms break up the bifurcation and thus the reported results (minimum, maximum and mean diameters and areas, RVD, percent diameter and area stenosis, length measurements) over a number of segments. This segmentation (Figure 3) facilitates more accurate localisation of minimum lumen diameter and thus more reliable late lumen loss measurements.

Beyond the diameter derived measures, an added piece of QCA derived information with significant impact on treatment strategy and outcome is the angulation between the main vessel and the SB[32]. The EBC has adopted a definition, according to which proximal and

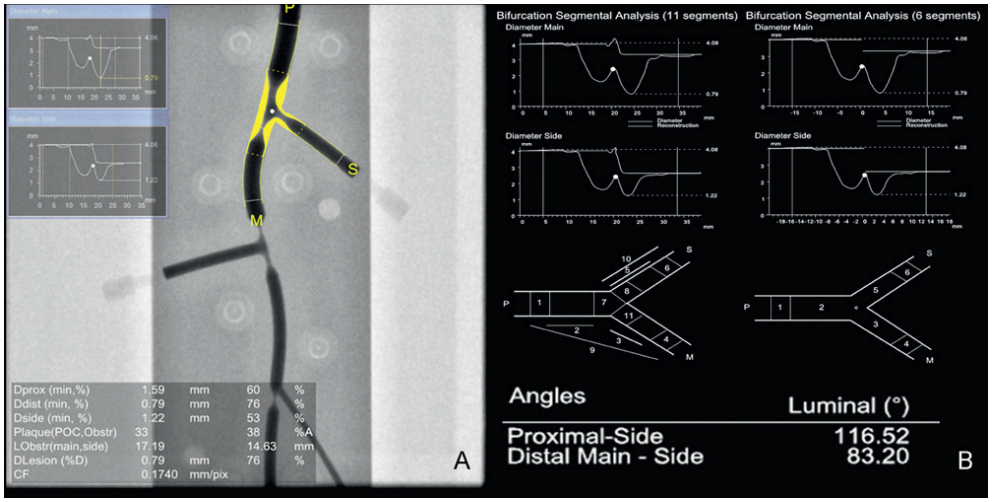

Figure 3. Analysis of a custom-made plexiglas phantom bifurcation; standard report of CAAS 5 (compilation). A. Analysed frame highlighting the plaque in yellow, with diameter graphs and numerical results for diameter-derived parameters for the 11-segment model. B. Upper panel: Single-point local reference obstruction analysis. Diameter graphs for main vessel and side branch for the 11- (left) and 6-segment (right) model. Middle panel: Model schematics. Lower panel: Bifurcation angle values.

distal bifurcation angle (BA) are delineated between the PMV and the SB, and between the DMV and the SB, respectively[21] (Figure 4). However, whereas BA calculations are carried out with digital calipers in QAngio XA, CAAS has developed a dedicated algorithm, applicable even in highly tortuous vessels, which adjusts for the diameter of the vessel segments at the POC boundaries. Shortly, vectors along the vessel segment centre lines are drawn, starting at the POC boundaries and directed either from distal to proximal (PMV) or from proximal to distal (DMV and SB). The size of the vectors, which can influence the BA calculation, is half the size of the equivalent luminal diameter at the proximal (PMV) or distal (DMV and SB) boundaries of the POC, respectively; this is based on the assumption that the curvature of the vessel is less than its radius. Proximal and distal angles are delineated between the respective vectors as already described.

Software validation

Until recently a validation of these dedicated software algorithms was lacking. For that purpose a series of six plexiglas phantoms were developed, each of them mimicking a vessel with three successive bifurcation lesions with variable anatomy and Medina class (Figure 5). Taking into account literature based specifications, the phantoms were designed using a computer aided program and manufactured using precision machining techniques[33]. Validation of the latest editions of the CAAS and QAngio XA presented during the sixth meeting of the European Bifurcation Club rendered highly accurate and precise results for MLD, RVD and DS measurements[34]. Additional validation of bifurcation QCA software algorithms was sought by re-examining the correlation with invasive functional testing. Until recently, QCA derived DS values in the SB ostium were deemed to be discordant with fractional flow reserve (FFR) measurements, either before or after stenting[8,35], as a result of applying single-vessel QCA algorithms to bifurcation lesions. A study by Sarno et al[36] on patients with bifurcations lesions, where angiograms and FFR pullbacks in both main vessel and SB were available, manifested a statistically significant inverse correlation of DS with FFR values both in the main vessel and the SB, when CAAS 2-D bifurcation QCA analysis was employed; conventional QCA resulted in a significant, however less powerful correlation only in the main vessel.

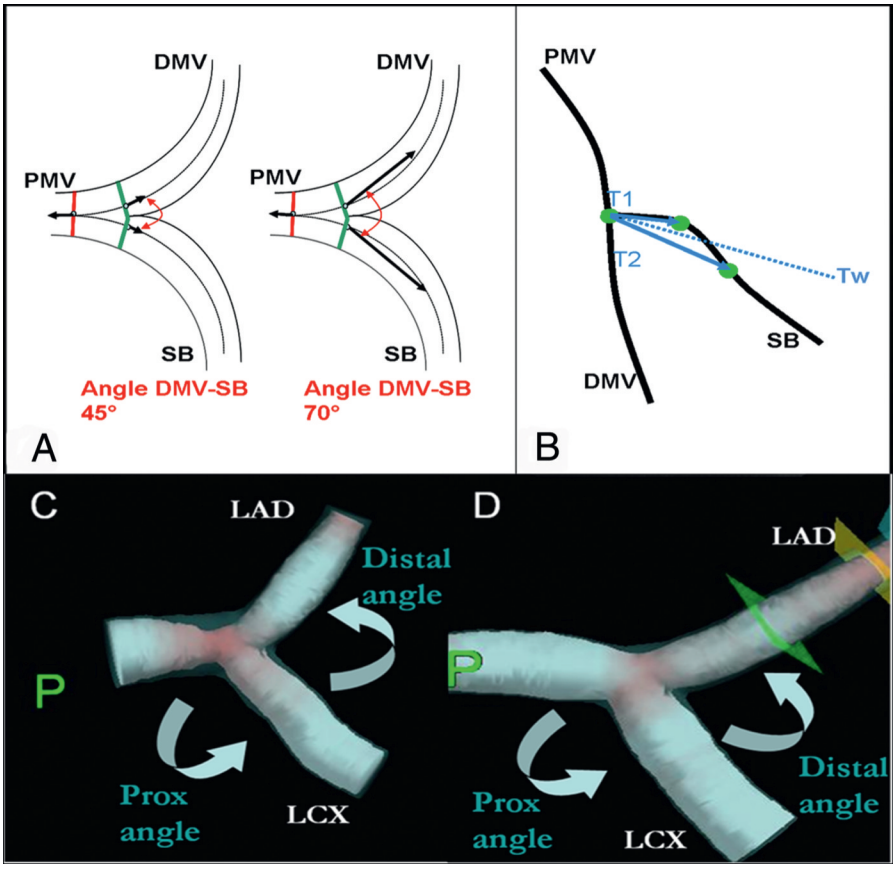

Figure 4. Bifurcation angle (BA) calculation. A. In CAAS, following the EBC definition, angles are delineated between vessel size adjusted vectors of direction; proximal BA between the proximal main vessel (PMV) and the side branch (SB), distal BA between the distal main vessel (DMV) and the SB. For different vector lengths, different angle values would be calculated. B. In CardiOp-B 3-D QCA algorithm, weighted vectors of direction are employed. The weighted vector (Tw) is calculated as the sum of two vectors, each of them connecting the junction point with distal points along the vessel centre line, distant by 5 mm (T1) and 10 mm (T2), respectively. C/D. BA calculation in a 3-D reconstructed distal left main bifurcation lesion before (C) and after treatment (D). The distal BA, delineated between the left anterior descending (LAD) and the left circumflex (LCX), gets narrower after treatment (CardiOp-B). EBC=European Bifurcation Club

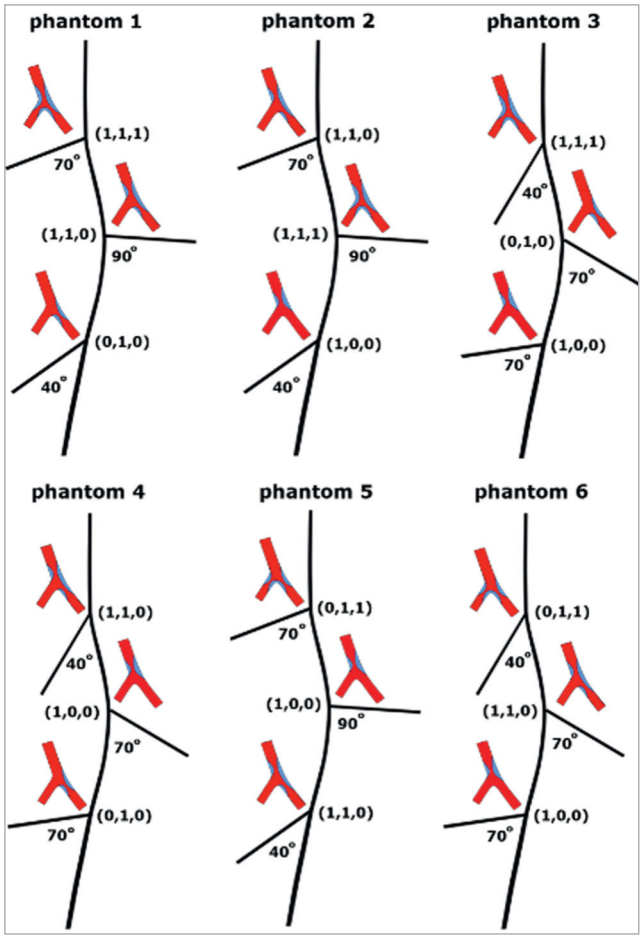

Figure 5. Schematic representation of the six plexiglas bifurcation phantoms used in the validation process. Medina class and side branch direction with respect to the distal main vessel are reported for each bifurcation.

3-D QCA

Accurate lesion assessment with 2-D QCA is limited by vessel overlap, foreshortening and out-of-plane magnification[37]. Inaccuracy in RVD, lesion length and BA determination coupled with suboptimal working projections may result in erroneous sizing and deployment of stents; this could translate into either incomplete lesion coverage and need for additional stents, or excessive stent length, jailing of a SB and increased restenosis rates[17,38-40].

Throughout the last 10 years, 3-D QCA software algorithms have been developed, that integrate two or more single-plane images, acquired by mono-plane or biplane system[15-17,40].

Most of them do not create a volumetric reconstruction of the true morphology of the vessel lumen, which still is computationally demanding and cannot be made available online, but rather a 3-D model, which is based on the reconstruction of 3-D center-line data; the diameter and 3-D structure of the vessel is subsequently derived with a computer algorithm.

The accuracy of these 3-D modelling algorithms heavily rely on the lack of geometric distortion on digital flat panels and the geometric information available from the DICOM headers of the angiographic system. Coronary 3-D reconstruction algorithms purely based on the 3-D system information, the so-called epipolar geometry reconstruction technique, provide only accurate reconstructions in those cases, where the vessel is roughly perpendicular to the X-ray beam[20]. A limitation of this technique is the erroneous assumption that the projected coronary artery from the acquired views is spatially identical[14,41]. In practice, even in biplane gantries, there is almost always an isocentre offset between planes due to system distortion (mainly gravity). Moreover due to (relatively large) respiratory motions and cardiac contraction motions, spatial correspondence between the two projections cannot be satisfied. In order to correct for the isocentre offset, we usually identify 1-3 pairs of reference points representing corresponding anatomical landmarks in the selected projections, for example bifurcation points. In order to correct for epipolar mismatch, dedicated 3-D geometric algorithms are employed; lastly ECG-gated, time adjusted frames from both acquisitions are combined into a 3-D reconstruction[20,40].

Notwithstanding subtle differences between available algorithms, a standard operator procedure for a 3-D reconstruction of a coronary lesion consists in the following four steps: 1. Two 2-D projections of the target vessel segment (possibly a bifurcation), separated by an angle ≥30°, with minimal foreshortening and overlap, are selected. 2. If needed, calibration on one of them is performed against the catheter[38]. However, full automatic calibration is the default (and only) choice in most algorithms. 3. In one of the projections, the target lesion is traced via the local contour detection algorithms; automatically a region of interest in the second 2-D image projection is indicated in order to assist the user in selecting the correct vessel segment within the second projection. 4. The 3-D model is created rendering an image and data on vessel diameter, lengths and angulation. Reduced time requirements (<60 sec for a single 3-D reconstruction) make the results readily available in real time.

Beyond graphic displays of the 3-D course and geometric relationship of vessels, quantification of foreshortening and overlap conditions allows the choice of an optimal view projection[40,42], notwithstanding constraints in gantry and patient positioning[37]. The accuracy of vessel length, diameter, and BA determination using 3-D modelling techniques has already been reported in several studies[14-18]. Bruining et al[43] in a quantitative multi-modality imaging analysis in patients receiving a bioabsorbable stent demonstrated the excellent correlation of 3-D QCA derived measurements for length and diameter with IVUS and multi-detector computed tomography; 2-D QCA showed significantly smaller stent lengths, whereas diameters and areas tended to be smaller as well. Tsuchida et al[44] and Ramcharitar et al[17] recently validated two commercially available 3-D QCA systems, CardiOp-B (Paieon Medical, Ltd., Rosh Ha'ayin, Israel) and CAAS 5 for single-vessel diameter and area measurements; CardiOp-B underestimated true values, CAAS 5 being more accurate and precise.

3-D bifurcation QCA algorithms

Both of these systems also incorporate dedicated 3-D bifurcation QCA algorithms, which allow sophisticated calculation of BA values following the EBC definition (Figure 4). CAAS 3-D QCA[20], while following the already described algorithm based on vessel size adjusted vectors, calculates BA values in 3-D space without

overlap, therefore theoretically more precisely than 2-D QCA. On the other hand, in CardiOp-B angle values were computed between the weighted vectors of direction of the respective vessel segments. The weighted vector is calculated as the sum of two vectors, each of them connecting the bifurcation point with distal (or proximal in the case of PMV) points along the vessel centre line, distant by 5 mm and 10 mm, respectively. This algorithm was employed in a recent substudy of the SYNTAX trial, the first ever to describe the 3-D angulation of the left main before and after intervention and its impact on 1-year clinical outcome[45].

When it comes to the quantification of stenosis, CardiOp-B provides diameter-derived and cross-sectional (densitometric) data together with the lesion length; lesion markers can be manipulated, in order to relocate the region of interest across the main vessel or from the PMV into the SB. In CAAS 5, a 3-D model of the central bifurcation area is constructed taking into account the fact that the contour information obtained from the 2-D projections may contain vessel overlap, since the bifurcated vessel might be partly obscured in at least one of the projections. To overcome this problem the 3-D cross-section shape is created using virtual vessel contours by virtue of information derived outside the bifurcation region (Figure 6)[20]. Cross-sectional area values are calculated on the assumption that the vessel has an elliptical cross section based on the luminal diameters from the two different 2-D projections; this elliptical cross-section is the primary measured parameter. The equivalent luminal diameter, minimum luminal diameter and maximal luminal diameter curves are calculated based on a circularity assumption. Reference vessel lines, up to the entrance of the POC and within the POC, are based on the 2-D approach adapted to 3-D.

Challenging cases

Notwithstanding these innovative software algorithms, there are two special situations in QCA analysis, which still need to be addressed; a diffusely diseased bifurcation region with no apparent healthy reference and an ostial stenosis in a short left main stem; it is not uncommon that both problems coincide in a single case. Based on the scaling laws of Murray and Finet, the size of any bifurcation vessel segment could be determined, if the reference of the other two vessel segments is known. This is not the case in a diffusely diseased bifurcation region; however, extrapolation of the reference of the PMV even on the basis of less accurate RVD values for the DMV and SB could avoid a gross underestimation of the PMV true size.

In the case of an ostial stenosis in a short left main stem, both contour detection and sizing could be challenging. Manual contour corrections would not be unreasonable, especially if there is overlap with the angiographic catheter. For the RVD determination, either a user-defined reference outside the obstructions boundaries but within the left main, or a value back-calculated from the distal branches reference values can be chosen (Figure 7). In both situations the experience of the analyst will be of apparent use.

References

1. Serruys PW, Wijns W, van den Brand M, Ribeiro V, Fioretti P, Simoons ML, Kooijman CJ, Reiber JH, Hugenholtz PG. Is transluminal coronary angioplasty mandatory after successful thrombolysis? Quantitative coronary angiographic study. *Br Heart J* 1983;50:257-65.

2. Reiber JH, Serruys PW, Kooijman CJ, Wijns W, Slager CJ, Gerbrands JJ, Schuurbiers JC, den Boer A, Hugenholtz PG. Assessment of short-, medium-, and long-term variations in arterial dimensions from computer-assisted quantitation of coronary cineangiograms. *Circulation* 1985;71:280-8.

3. Serruys PW, Kay IP, Disco C, Deshpande NV, de Feyter PJ. Periprocedural quantitative coronary angiography after Palmaz-Schatz stent implantation predicts the restenosis rate at six months: results of a meta-analysis of the BElgian NEtherlands Stent study (BENESTENT) I, BENESTENT II Pilot, BENESTENT II and MUSIC trials. Multicenter Ultrasound Stent In Coronaries. *J Am Coll Cardiol* 1999;34:1067-74.

4. Mauri L, Orav EJ, Kuntz RE. Late loss in lumen diameter and binary restenosis for drug-eluting stent comparison. *Circulation* 2005;111:3435-42.

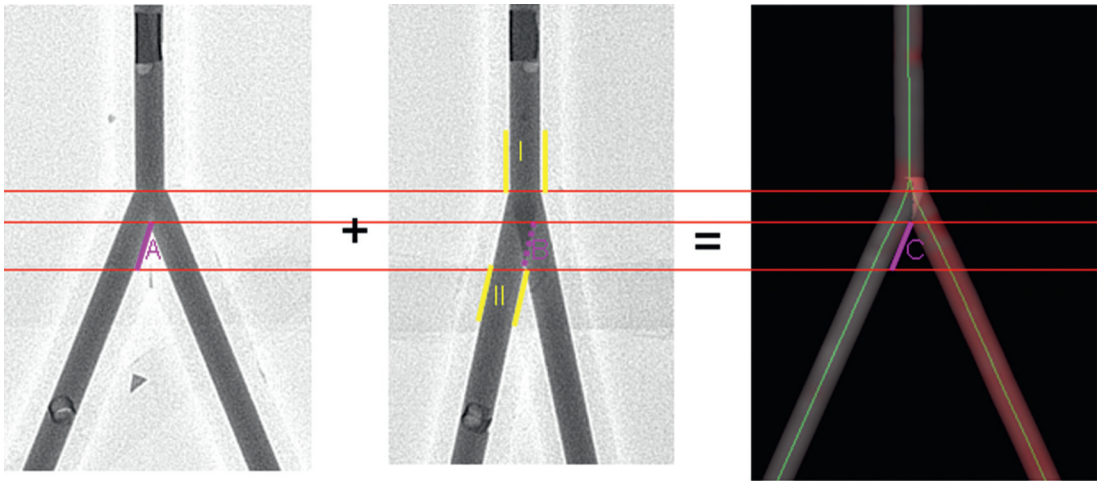

Figure 6. CAAS 3-D solution for vessel overlap in 2-D images of a bifurcation. Contour A is visible but contour B is hidden in the second 2-D image due to overlap. Missing contour B is determined from region I (proximal main vessel) and region II (distal branch) using "spline" interpolation. In the 3-D reconstruction contour C is then calculated from contours A and B.

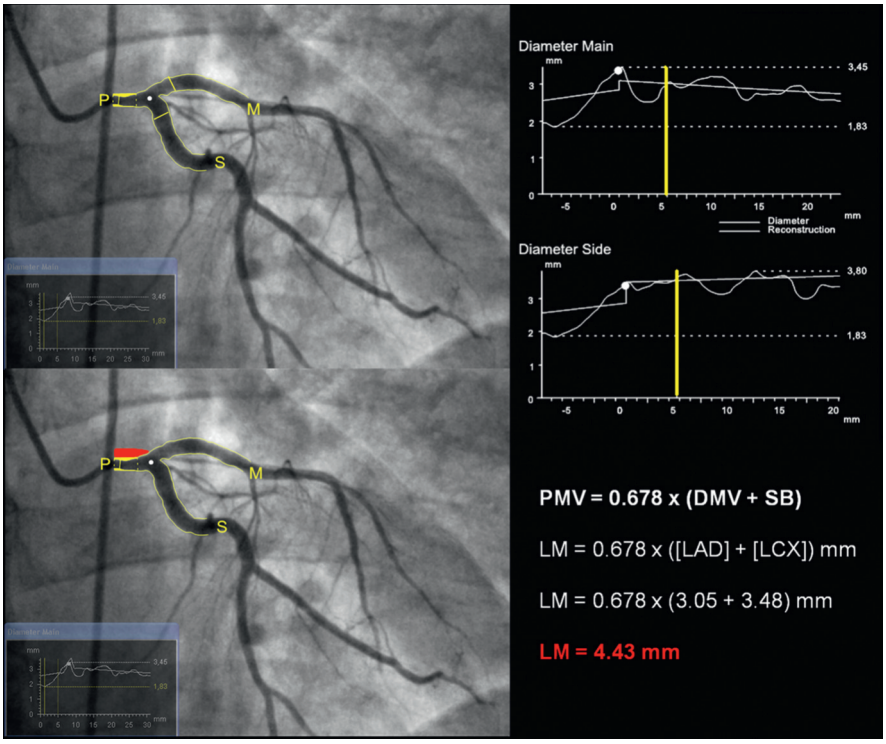

Figure 7. Reference obstruction analysis in a diffusely diseased left main. In the upper image plaque is highlighted in yellow reflecting the results of automatic reference obstruction analysis; a gross underestimation of the left main expected dimensions is evident both on the angiographic image and on the diameter graphs. To compensate for the lack of a healthy reference point within the left main, an approximated reference value can be derived based on the scaling law by Finet, given the reference diameter in the distal main vessel (M) and in the side branch (S). In the lower image, the true size of the left main obstruction is approximated after the addition of the red area on top of the already traced plaque burden.

5. Pocock SJ, Lansky AJ, Mehran R, Popma JJ, Fahy MP, Na Y, Dangas G, Moses JW, Pucelikova T, Kandzari DE and others. Angiographic surrogate end points in drug-eluting stent trials: a systematic evaluation based on individual patient data from 11 randomized, controlled trials. *J Am Coll Cardiol* 2008;51:23-32.

6. Zijlstra F, van Ommeren J, Reiber JH, Serruys PW. Does the quantitative assessment of coronary artery dimensions predict the physiologic significance of a coronary stenosis? *Circulation* 1987;75:1154-61.

7. Zijlstra F, Fioretti P, Reiber JH, Serruys PW. Which cineangiographically assessed anatomic variable correlates best with functional measurements of stenosis severity? A comparison of quantitative analysis of the coronary cineangiogram with measured coronary flow reserve and exercise/redistribution thallium-201 scintigraphy. *J Am Coll Cardiol* 1988;12:686-91.

8. Koo BK, Kang HJ, Youn TJ, Chae IH, Choi DJ, Kim HS, Sohn DW, Oh BH, Lee MM, Park YB and others. Physiologic assessment of jailed side branch lesions using fractional flow reserve. *J Am Coll Cardiol* 2005;46:633-7.

9. Goktekin O, Kaplan S, Dimopoulos K, Barlis P, Tanigawa J, Vatankulu MA, Koning G, Tuinenburg JC, Mario CD. A new quantitative analysis system for the evaluation of coronary bifurcation lesions: comparison with current conventional methods. *Catheter Cardiovasc Interv* 2007;69:172-80.

10. Ramcharitar S, Onuma Y, Aben JP, Consten C, Weijers B, Morel MA, Serruys PW. A novel dedicated quantitative coronary analysis methodology for bifurcation lesions. *EuroIntervention* 2008;3:553-7.

11. Lansky A, Tuinenburg J, Costa M, Maeng M, Koning G, Popma J, Cristea E, Gavit L, Costa R, Rares A and others. Quantitative angiographic methods for bifurcation lesions: a consensus statement from the European Bifurcation Group. *Catheter Cardiovasc Interv* 2009;73:258-66.

12. Girasis C, Schuurbiers JC, Onuma Y, Aben JP, Weijers B, Boersma E, Wentzel JJ, Serruys PW. Two-dimensional quantitative coronary angiographic models for bifurcation segmental analysis: In vitro validation of caas against precision manufactured plexiglas phantoms. *Catheter Cardiovasc Interv* 2010; in press.

13. Green NE, Chen SY, Messenger JC, Groves BM, Carroll JD. Three-dimensional vascular angiography. *Curr Probl Cardiol* 2004;29:104-42.

14. Wellnhofer E, Wahle A, Mugaragu I, Gross J, Oswald H, Fleck E. Validation of an accurate method for three-dimensional reconstruction and quantitative assessment of volumes, lengths and diameters of coronary vascular branches and segments from biplane angiographic projections. *Int J Card Imaging* 1999;15:339-53; discussion 355-6.

15. Messenger JC, Chen SY, Carroll JD, Burchenal JE, Kioussopoulos K, Groves BM. 3D coronary reconstruction from routine single-plane coronary angiograms: clinical validation and quantitative analysis of the right coronary artery in 100 patients. *Int J Card Imaging* 2000;16:413-27.

16. Dvir D, Marom H, Guetta V, Kornowski R. Three-dimensional coronary reconstruction from routine single-plane coronary angiograms: in vivo quantitative validation. *Int J Cardiovasc Intervent* 2005;7:141-5.

17. Ramcharitar S, Daeman J, Patterson M, van Guens RJ, Boersma E, Serruys PW, van der Giessen WJ. First direct in vivo comparison of two commercially available three-dimensional quantitative coronary angiography systems. *Catheter Cardiovasc Interv* 2008;71:44-50.

18. Schuurbiers JC, Lopez NG, Ligthart J, Gijsen FJ, Dijkstra J, Serruys PW, Van der Steen AF, Wentzel JJ. In vivo validation of CAAS QCA-3D coro-

nary reconstruction using fusion of angiography and intravascular ultrasound (ANGUS). *Catheter Cardiovasc Interv* 2009;73:620-6.

19. Schlundt C, Kreft JG, Fuchs F, Achenbach S, Daniel WG, Ludwig J. Three-dimensional on-line reconstruction of coronary bifurcated lesions to optimize side-branch stenting. *Catheter Cardiovasc Interv* 2006;68:249-53.

20. Onuma Y, Girasis C, Aben JP, Sarno G, Piazza N, Lokkerbol C, Morel MA, Serruys PW. A novel dedicated 3-dimensional quantitative coronary analysis methodology for bifurcation lesions. *EuroIntervention* 2010; in press.

21. Louvard Y, Thomas M, Dzavik V, Hildick-Smith D, Galassi AR, Pan M, Burzotta F, Zelizko M, Dudek D, Ludman P and others. Classification of coronary artery bifurcation lesions and treatments: time for a consensus! *Catheter Cardiovasc Interv* 2008;71:175-83.

22. Medina A, Suarez de Lezo J, Pan M. A new classification of coronary bifurcation lesions. *Rev Esp Cardiol* 2006;59:183.

23. Serruys PW, Reiber JH, Wijns W, van den Brand M, Kooijman CJ, ten Katen HJ, Hugenholtz PG. Assessment of percutaneous transluminal coronary angioplasty by quantitative coronary angiography: diameter versus densitometric area measurements. *Am J Cardiol* 1984;54:482-8.

24. Scoblionko DP, Brown BG, Mitten S, Caldwell JH, Kennedy JW, Bolson EL, Dodge HT. A new digital electronic caliper for measurement of coronary arterial stenosis: comparison with visual estimates and computer-assisted measurements. *Am J Cardiol* 1984;53:689-93.

25. Katritsis D, Lythall DA, Anderson MH, Cooper IC, Webb-Peploe MW. Assessment of coronary angioplasty by an automated digital angiographic method. *Am Heart J* 1988;116:1181-7.

26. Detre KM, Wright E, Murphy ML, Takaro T. Observer agreement in evaluating coronary angiograms. *Circulation* 1975;52:979-86.

27. Zir LM, Miller SW, Dinsmore RE, Gilbert JP, Harthorne JW. Interobserver variability in coronary angiography. *Circulation* 1976; 53:627-32.

28. DeRouen TA, Murray JA, Owen W. Variability in the analysis of coronary arteriograms. *Circulation* 1977;55:324-8.

29. Girasis C, Onuma Y, Schuurbiers JC, Morel MA, Wentzel JJ, Serruys PW. Visual Assessment of Stenosis Severity in Phantom Bifurcation Lesions: A Survey in Experts 2009; Berlin.

30. Huo Y, Kassab GS. A scaling law of vascular volume. *Biophys J* 2009;96:347-53.

31. Finet G, Gilard M, Perrenot B, Rioufol G, Motreff P, Gavit L, Prost R. Fractal geometry of arterial coronary bifurcations: a quantitative coronary angiography and intravascular ultrasound analysis. *EuroIntervention* 2008;3:490-8.

32. Dzavik V, Kharbanda R, Ivanov J, Ing DJ, Bui S, Mackie K, Ramsamujh R, Barolet A, Schwartz L, Seidelin PH. Predictors of long-term outcome after crush stenting of coronary bifurcation lesions: importance of the bifurcation angle. *Am Heart J* 2006;152:762-9.

33. Girasis C, Schuurbiers JC, Onuma Y, Serruys PW, Wentzel JJ. Novel bifurcation phantoms for validation of quantitative coronary angiography algorithms. *Catheter Cardiovasc Interv* 2010; in press.

34. Girasis C, Serruys PW. Dedicated Software for Bifurcation QCA: Pie Medical (CAAS 5.9) and MEDIS (QAngio XA 7.2.34.0) Validation on Phantom analysis. 2010; Budapest.

35. Koo BK, Park KW, Kang HJ, Cho YS, Chung WY, Youn TJ, Chae IH, Choi DJ, Tahk SJ, Oh BH and others. Physiological evaluation of the provisional side-branch intervention strategy for bifurcation lesions using fractional flow reserve. *Eur Heart J* 2008;29:726-32.

36. Sarno G, Garg S, Onuma Y, Girasis C, Tonino P, Morel MA, Van Es GA, Pijls N, Serruys PW. Bifurcation lesions: Novel anatomical evaluation by Quantitative Coronary Angiogram versus functional assessment by Fractional Flow Reserve. *Cathet Cardiovasc Interv* 2010;submitted.

37. Green NE, Chen SY, Hansgen AR, Messenger JC, Groves BM, Carroll JD. Angiographic views used for percutaneous coronary interventions: a three-dimensional analysis of physician-determined vs. computer-generated views. *Catheter Cardiovasc Interv* 2005;64:451-9.

38. Gollapudi RR, Valencia R, Lee SS, Wong GB, Teirstein PS, Price MJ. Utility of three-dimensional reconstruction of coronary angiography to guide percutaneous coronary intervention. *Catheter Cardiovasc Interv* 2007;69:479-82.

39. Sadamatsu K, Sagara S, Yamawaki T, Tashiro H. Three-dimensional coronary imaging for the ostium of the left anterior descending artery. Int *J Cardiovasc Imaging* 2009;25:223-8.

40. Tu S, Koning G, Jukema W, Reiber JH. Assessment of obstruction length and optimal viewing angle from biplane X-ray angiograms. *Int J Cardiovasc Imaging* 2010;26:5-17.

41. Wahle A, Wellnhofer E, Mugaragu I, Saner HU, Oswald H, Fleck E. Assessment of diffuse coronary artery disease by quantitative analysis of coronary morphology based upon 3-D reconstruction from biplane angiograms. *IEEE Trans Med Imaging* 1995;14:230-41.

42. Garcia JA, Movassaghi B, Casserly IP, Klein AJ, Chen SY, Messenger JC, Hansgen A, Wink O, Groves BM, Carroll JD. Determination of optimal viewing regions for X-ray coronary angiography based on a quantitative analysis of 3D reconstructed models. *Int J Cardiovasc Imaging* 2009;25:455-62.

43. Bruining N, Tanimoto S, Otsuka M, Weustink A, Ligthart J, de Winter S, van Mieghem C, Nieman K, de Feyter PJ, van Domburg RT and others. Quantitative multi-modality imaging analysis of a bioabsorbable poly-L-lactic acid stent design in the acute phase: a comparison between 2- and 3D-QCA, QCU and QMSCT-CA. *EuroIntervention* 2008;4:285-91.

44. Tsuchida K, van der Giessen WJ, Patterson M, Tanimoto S, Garcia-Garcia HM, Regar E, Ligthart JM, Maugenest AM, Maatrijk G, Wentzel JJ and others. In vivo validation of a novel three-dimensional quantitative coronary angiography system (CardiOp-B): comparison with a conventional two-dimensional system (CAAS II) and with special reference to optical coherence tomography. *EuroIntervention* 2007;3:100-8.

45. Girasis C, Serruys PW, Onuma Y, Colombo A, Holmes DR, Jr., Feldman TE, Bass EJ, Leadley K, Dawkins KD, Morice MC. 3-Dimensional Bifurcation Angle Analysis in Patients With Left Main Disease A Substudy of the SYNTAX Trial (SYNergy Between Percutaneous Coronary Intervention With TAXus and Cardiac Surgery). *JACC Cardiovasc Interv* 2010;3:41-48.